Hindawi
Journal of Food Quality
Volume 2023, Article ID 8566804, 8 pages
https://doi.org/10.1155/2023/8566804

Research Article

Effects of Mannitol and Xylitol on the Quality of Spicy Wheat Gluten Sticks

Qiuyan Ren,[1,2] Heng Yang,[3] Ziyang Jia,[1,2] Wenping Ding,[1,2] Yang Fu,[1,2] Shensheng Xiao,[1,2] Yanmei Wei,[1,2] Kaifeng Zhao,[1,2] Yan Wu,[1,2] and Xuedong Wang[1,2]

[1]*Hubei Key Laboratory for Processing and Transformation of Agricultural Products, Wuhan Polytechnic University, Wuhan, China*
[2]*Key Laboratory for Deep Processing of Major Grain and Oil, Ministry of Education, Wuhan Polytechnic University, Wuhan, China*
[3]*Angel Yeast Co., Ltd., 168 Chengdong Avenue, Yichang, Hubei, China*

Correspondence should be addressed to Yan Wu; wuyan23@163.com and Xuedong Wang; xuedongwuhan@163.com

Received 5 May 2023; Revised 30 August 2023; Accepted 14 September 2023; Published 28 September 2023

Academic Editor: Mohamed Addi

The present study sought to evaluate the effects and mechanisms of mannitol and xylitol on the regeneration of spicy wheat gluten sticks (SWGSs) through texture profile analysis (TPA), Fourier-transform infrared spectroscopy (FTIR), differential scanning calorimetry (DSC), X-ray diffraction (XRD), and low-field nuclear magnetic resonance (LF-NMR). The rate constant of crystallization and the relative degree of crystallinity of SWGS substantially reduced with polyols addition after 4 weeks of storage at 4°C. The peaks near 3385 cm^{-1} and 1081 cm^{-1} in FTIR of SWGS became wider with the addition of mannitol and xylitol, indicating that mannitol and xylitol formed hydrogen bonds by binding to wheat starch. The DSC experiment results showed that the addition of mannitol and xylitol could reduce the T_p and ΔH of SWGS powder effectively under different storage times. The NMR results showed that the water in SWGS was mainly immobile water, and the addition of mannitol and xylitol could increase the content of bound water and immobile water in SWGS and reduce the water migration. These results provided deeper insights into the action mechanism of mannitol and xylitol in delaying the quality change of starch products during storage, thereby providing a reference for inhibiting SWGS regeneration. Therefore, it could be inferred that improving the quality of SWGS by adding polyol might have significant application prospects in the food industry.

1. Introduction

Wheat is the world's second most essential grain after rice [1], with a global production of 772 million metric tons by 2020/2021. Wheat is often used as a raw material for making bread, cakes, biscuits, and other baked foods [2]. Of them, the spicy wheat gluten sticks made by thorough mixing of raw and auxiliary materials, such as wheat flour, salt, and water, followed by extrusion, are popular among young people in China. During the processing of extruded noodle products, a driving force is generated by the rotation of the extruder screw constantly, which helps the mixture turn over with the rotation of the screw. Meanwhile, the mixture and the barrel wall are mixed and compressed due to friction and collision, which increases the pressure and temperature in the barrel, thereby activating the molten state of the mixture. As it passes through the mold, the pressure drops dramatically, the internal water evaporates, and the starch expands significantly, leading to the forming of a microporous structure and the formation of a spicy bran bar [3].

As a starchy food, the spicy wheat gluten sticks (SWGSs) are gelatinized under high-temperature treatment and water, allowing the particles to absorb water and expand. Water absorption leads to the collapse of particles and derangement of polymer chains. The amorphous chain undergoes hydrophobic interaction and rearrangement upon cooling down of the superheating system, which adversely affects the product quality [4]. Starch retrogradation severely affects the

texture, flavor, shelf life, and nutritional value of starch-based products [5]. In the food industry, many additives are used to delay starch retrogradation. For instance, *Laminaria japonica* polysaccharides may form more hydrogen bonds and interfere with starch reassociation and retrogradation in bread [6]. Green tea polyphenols reduce the pasting properties of rice starch by facilitating the hydration of starch granules, building a cross-linking association between starch granules, and decreasing the peak temperature and gelatinization enthalpy [7]. However, these additives are unstable under high temperatures and pressure and are not suitable for SWGS production.

Polyols are a class of carbohydrates with multiple hydroxyl groups, possessing good water-holding properties, and are often used in food processing. It is reported that the water retention capacity of polyols and their interaction with gluten proteins and the gluten network in fresh noodles containing low molecular weight polyols are highly resistant to water migration and deformation during storage [8]. The addition of maltitol could reduce water migration in bread, the loss of water in bread, and maintain the softness of bread [9]. Similarly, xylitol could effectively prolong the shelf life of bread, maintain the softness of bread, and improve the storage quality of bread. Our previous studies have reported the effects of polyols on wheat starch retrogradation [10].

To the best of our knowledge, this is the first study to report the antiretrogradation effect of polyols on starch foods so far. The present study aimed at evaluating the antiretrogradation effect of mannitol and xylitol on SWGS and the retrogradation characteristics of mannitol and xylitol on SWGS at different storage times. In addition, the influence mechanism of polyols (mannitol or xylitol) on SWGS retrogradation was explored through texture profile analysis (TPA), Fourier-transform infrared spectroscopy (FTIR), differential scanning calorimetry (DSC), X-ray diffraction (XRD), and low-field nuclear magnetic resonance (LF-NMR). Overall, the study results revealed the relationship between food composition structure and starch retrogradation, providing insights into the processing of starch-based products.

2. Materials and Methods

2.1. Materials. The wheat flour used to produce SWGS was purchased from A Natural Flour Co. Ltd. (Zhumadian, China), with moisture content, ash content, and crude protein content of 13.34 wt%, 0.75 wt%, and 11.26 wt%, respectively. Mannitol (99% purity) and xylitol (99.5% purity) were purchased from Hunan Xinlvfang Pharmaceutical Co., Ltd. and Zhejiang Huakang Pharmaceutical Co., Ltd., respectively.

2.2. Preparation of SWGS. The SWGS mainly consisted of 25000 g of wheat flour, 0.6% monoglyceride, 6% salt, and 30% water. In addition, 0–5% mannitol or 0–5% xylitol was added to the flour as an additive. The flour, monoglyceride, salt, and water were mixed using a drum powder machine (Pingjiang Hongyu Machinery Manufacturing Co., Ltd., Yueyang, China). The mixture was cast using a single screw extruder (Pingjiang Hongyu Machinery Manufacturing Co., Ltd.). The first feeding speed was 500 g/min, and the feeding speed was adjusted to 1800 g/min slowly after the SWGS coming out of the machine. The sample was placed on the conveyor belt and cut into a 15 cm length. The moisture content of SWGS varied with the addition of different contents of mannitol and xylitol, ranging from 25.0% to 27.0%. Later, it was cooled down at room temperature for 2 min and packaged with sealed bags. Finally, the SWGS were stored at 25°C for 0, 1, 2, 3, and 4 weeks.

2.3. Texture Profile Analysis. The textural analysis of SWGS was performed by using a TA.TOUCH Texture Analyzer (Shanghai Baosheng Industrial Development Co., Ltd.) equipped with a TA/LKB probe, according to the previously reported method [11]. The test conditions were as follows: pretest speed of 1.0 mm/s, a test speed of 2.0 mm/s, a posttest speed of 2.0 mm/s, a distance of 20.0 mm, and a trigger force of 100 N. All experiments were repeated 15 times.

2.4. Fourier-Transform Infrared Spectroscopy. The FTIR analysis was performed according to the previously reported method with slight modifications [12]. The mixture of starch and dried potassium bromide was prepared using an agate mortar and stirred at 1 : 100 mass ratios. After grinding, the sample was pressed into flakes and placed on the sample holder of the FTIR spectrometer (Nicolette Instruments, USA). The spectra were set between 400 cm^{-1} and 4000 cm^{-1} using a pure potassium bromide tablet as the background and scanned 32 times at 4 cm^{-1} resolution.

2.5. X-Ray Diffraction. The wide angle X-ray diffraction patterns of retrograded starch powder were determined using an X-ray diffractometer (PANalytical B.V., Netherlands), according to the previously reported method, with minor modifications [13]. This test was conducted at room temperature with a scan rate of 2°/min and a diffraction angle range of 4–50°. The target voltage and current were 45 kV and 40 mA, respectively. The relative crystallinity (RC) of the samples was calculated according to equation (1) and analyzed by using Jade 6 software.

$$\text{Rc}\ (\%) = \frac{\text{Ac}}{\text{Ac} + \text{Aa}} * 100, \quad (1)$$

where Ac is the crystalline area and Aa is the amorphous areas.

2.6. Differential Scanning Calorimetry (DSC). The thermal properties were measured by a differential scanning calorimeter (TA Instruments, USA) in an ultrahigh purity nitrogen environment. About 3 mg of starch powder was accurately weighed into aluminum DSC trays. The heat sweep was performed from 35°C to 245°C at a constant heating rate of 15°C/min [14]. Later, the transition temperatures (To and Tc) and total transition enthalpy changes

(ΔH) were recorded. The kinetic properties of starch retrogradation were explored using the *Avrami* equation [15]:

$$R = 1 - \exp^{-kt^n}, \quad (2)$$

where R is the crystallization ratio of starch at time t, k is the rate constant, and n is the *Avrami* exponent.

In the DSC test, R was calculated using the following equation:

$$R = \frac{\triangle H_t - \triangle H_0}{\triangle H_\infty - \triangle H_0}, \quad (3)$$

where ΔH_0 and ΔH_t are the enthalpy transitions formed at time 0 and time t, respectively (for the purposes of this study ΔH_0 is zero), as ΔH_∞ was the limiting value of the change in enthalpy (4 weeks for all samples).

Equation (4) is the combination and simplification of equations (2) and (3).

$$\ln\left[-\ln\left(1 - \frac{\triangle H_t}{\triangle H_\infty}\right)\right] = n\ln t + \ln k. \quad (4)$$

2.7. Low-Field Nuclear Magnetic Resonance. The LF-NMR experiments (Suzhou Newmark Analytical Instruments Co., Ltd.) were performed according to the previously reported method with minor modifications [16]. In order to prevent water loss during storage, the prepared samples (as described in Section 2.3) were transferred to an NMR glass tube (18 mm in diameter) and sealed using parafilm. The tubes were stored for 0, 1, 2, 3, and 4 weeks at 4°C. The retrograded starches were equilibrated at room temperature (25°C) for 1 h before measurement. The spin-spin relaxation time (T_2) was determined using the Carr–Purcell–Meiboom–Gill (CPMG) sequence. As for CPMG sequence, the number of echoes was 4 and the number of sweeps (Ns) was 8.

2.8. Statistical Analysis. All the experiments were performed in triplicate using a completely randomized design to calculate the average and standard deviation. The curve was plotted by using ORIGIN 8.5 (Origin Lab Inc.), and the data were analyzed by one-way analysis of variance and Duncan's multiple range test ($p < 0.05$) using SPSS 19.0 (SPSS Inc.).

3. Results and Discussion

3.1. Texture Profile Analysis. Texture analysis is an analytical method used to evaluate the performance of SWGS by simulating the chewing process, in which hardness plays a vital role in determining food quality [17]. As for SWGS, the firmness and chewiness were used to mirror the texture of the product. The low hardness and good chewiness indicated good quality SWGS.

Figure 1 shows the changes in the hardness of SWGS stored for 0, 1, 2, 3, and 4 weeks at 4°C with and without mannitol and xylitol. The hardness of SWGS increased with increased storage times, which could be mainly attributed to the retrogradation of wheat starch during storage [18].

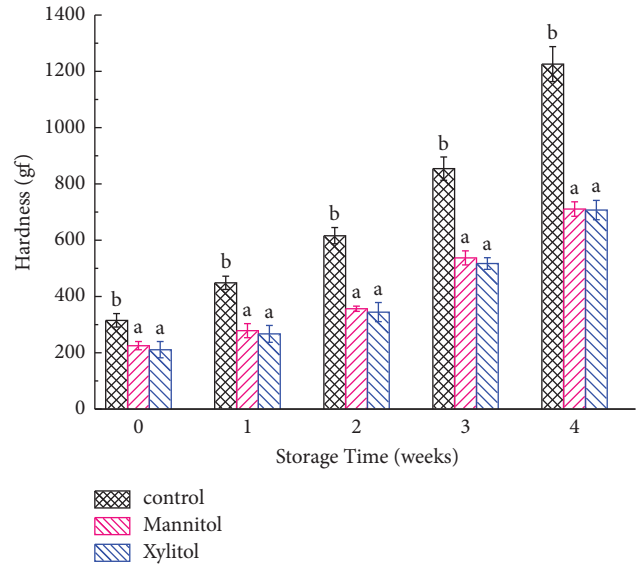

Figure 1: Changes in the hardness of SWGS stored for 0, 1, 2, 3, and 4 weeks at 4°C.

Meanwhile, high-density crystalline molecules were formed during starch retrogradation. The crystallinity of starch significantly increased with increased storage time, thereby increasing the hardness [19]. The addition of 2% mannitol and 4% xylitol significantly decreased the hardness of SWGS by 42.0% and 42.3%, respectively. This might be attributed to hydroxyl structures of the mannitol and xylitol that formed hydrogen bonds with starch. The binding between the starches prevented the formation of a double-helix structure and inhibited the rearrangement of starch molecules [20]. These results suggested that the addition of mannitol and xylitol might inhibit starch retrogradation, which was consistent with the results of previous studies reporting that the interaction of starch and xylitol could limit the recrystallization of wheat starch [21]. In addition, mannitol and xylitol reduced the free water content in the system by combining with water through hydrogen bonds and significantly prevented water loss, thus maintaining the softness of SWGS [22].

The *Avrami* equation describing the time dependence of crystal growth over time during polymer crystallization is widely used in the study of starch retrogradation kinetic models. The recrystallization kinetics of starch was calculated using the *Avrami* equation and expressed by R [23] as follows:

$$R = \frac{F_t - F_0}{F_\infty - F_0} = 1 - \exp^{-kt^n}, \quad (5)$$

where R represents the percentage of starch crystallization to the total limit of crystallization at time t/%; F_0, F_∞, and F_t are the hardness of SWGS at zero time, ∞, and "t" time; k is a rate constant (this usually takes for the form of $1/k$ = time constant to compare firming rate); and n is the *Avrami* exponent, a characteristic related to the nucleation of crystallites and their subsequent growth.

Equation (5) was obtained by equation (6):

$$\ln\left[-\ln\left(1-\frac{F_t-F_0}{F_\infty-F_0}\right)\right]=n\ln t+\ln k. \quad (6)$$

Here, the rate of retrogradation of SWGS was calculated using the hardness of the products instead of the starch regeneration crystallization rate; n is the *Avrami* index and depends on the nucleation mode in the crystal; k is the crystallization rate constant, which represents the crystal growth rate; R is the degree to which the equation fits [24].

As can be seen from Table 1, the R^2 of the *Avrami* equation of all samples was close to 1, confirming the suitability of the *Avrami* equation to explain the retrogradation behavior. In the Avrami equation, the *Avrami* index n below 1 suggests the crystallization growth process to be instantaneous nucleation, and when n is above 1, the crystallization nucleation mode is spontaneous nucleation [25]. Here, the *Avrami* exponent was $n<1$, indicating that the nucleation of starch crystals in SWGS was instantaneous. These results were consistent with previous study results, reporting that the basic mechanism of starch crystallization was transient nucleation followed by linear crystal growth [26]. Most crystallization occurred during the first storage phase, indicating that starch retrogradation increased during the earlier phases and decreased during the later phases of storage. Compared to the blank SWGS, the k-values of SWGS with mannitol and xylitol were lower, being minimal in SWGS with xylitol, and stored for 4 weeks at 4°C than the other groups. The SWGS with xylitol showed a minimum k-value after 4 weeks of storage at 4°C, which decreased from 0.150 and 0.107 to 0.053 and 0.066, respectively. The abovementioned results proved that the addition of xylitol could inhibit the retrogradation of SWGS more effectively than mannitol.

3.2. Fourier-Transform Infrared Spectroscopy. FTIR could observe the changes in the intensity and position of characteristic peaks in starch and enable the analysis of conformational changes in the molecular structure of starch granules [27]. Figure 2 shows the effect of the addition of mannitol and xylitol on the FTIR profiles of SWGS lyophilized powders. All the SWGS produced absorption peaks from 400 to 4000 cm^{-1} during storage. For each sample, broad and strong infrared absorption peaks were seen in the range of 3385 cm^{-1}, which represented the –OH stretching vibration inside the starch. The band representing the internal –OH stretching vibration of starch was observed near 3385 cm^{-1}, and the formation of hydrogen bonds coincided with this phenomenon [28]. As for the samples with mannitol and xylitol, the peaks at 3385 cm^{-1} were broadened and of high intensity. This might be attributed to the interaction of the multiple hydroxyl moieties in both mannitol and xylitol with the starch [29]. This phenomenon impeded the interaction between the starches and resulted in a change in the starch structure during retrogradation.

The characteristic spectral features of starch were in the range of 800–1300 cm^{-1}, which were sensitive to the conformational and crystalline structure of starch. The –OH bending vibration of the polymer was signified by an absorption band located around 1081 cm^{-1}, indicating that a hydrogen bond was established [20]. The samples with mannitol and xylitol showed significantly wider and higher peak –OH bands than the blanks, which might be attributed to the increase in the swelled amorphous region and the chain segments on the crystalline surface. These chain segments interacted with amylose in the heterogeneous systems [30]. Notably, stronger hydrogen bonds were observed between the molecules, which prevented the interaction of amylose-amylose and reduced the network structure formation in the continuous phase. Finally, the addition of mannitol and xylitol significantly decreased the hydrogen bonding between amylose-amylose in the SWGS, thereby decreasing the retrogradation of SWGS.

Table 1: Effect of mannitol and xylitol on the kinetic parameters of SWGS.

Sample	Avrami	n	lnk	k	R^2
Control	$y=0.618x-1.900$	0.618	−1.900	0.150	0.950
Mannitol	$y=0.675x-2.984$	0.675	−2.984	0.051	0.925
Xylitol	$y=0.647x-2.938$	0.647	−2.938	0.053	0.926

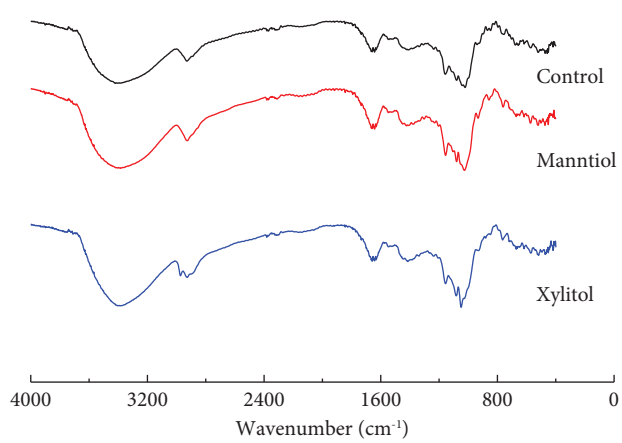

Figure 2: Effects of mannitol and xylitol on the FTIR spectra of SWGS.

3.3. X-Ray Diffraction. Figure 3 shows the X-ray diffraction diagrams of fresh and stored SWGS for 4 weeks, with a distinct peak at 2θ~13°, 20°, which was a typical V-shaped structure of starch. V-shaped amylose is a compound in the form of a left-handed helix produced by the interaction of amylose with several small molecules. The SWGS peak at 2θ~13° could be attributed to the monoglycerides, the raw material used to prepare SWGS, which may also form a V-shaped starch structure [31]. When mannitol or xylitol was added to the sample, the position of diffraction peaks was not altered, nor was the type of starch crystallization affected. During pasting, the semicrystalline structure of the starch granules is transformed into an amorphous form, and subsequently, the dextrinized starch is to reconnect with an ordered crystalline structure during regeneration. Consequently, the relative crystallinity of the starch after pasting is lower than that of natural starch [32].

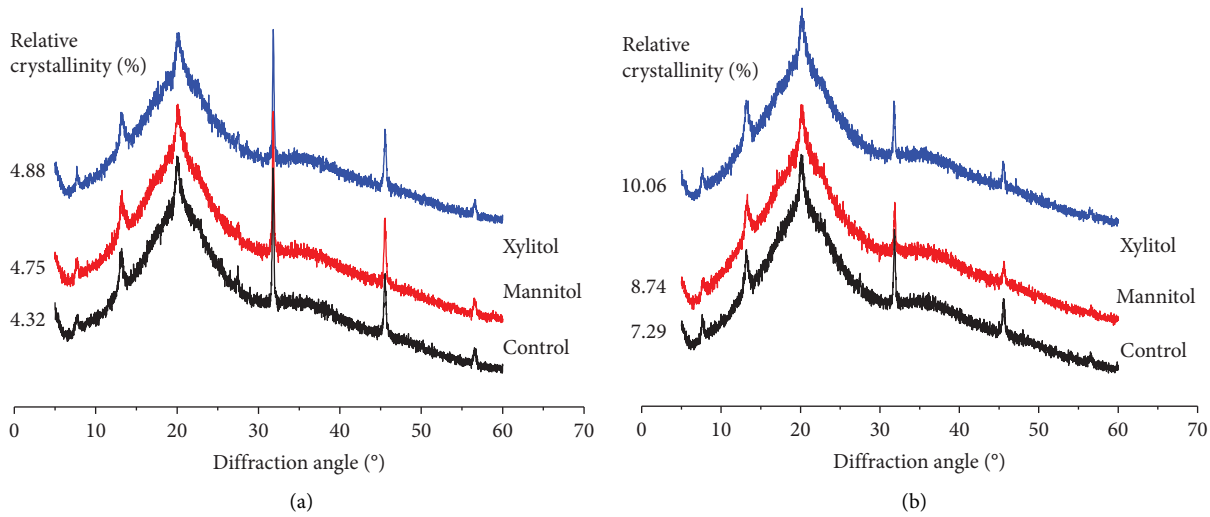

Figure 3: Effects of mannitol and xylitol on XRD diffraction pattern of SWGS stored at 4°C for 0 (a) and 4 (b) weeks.

The crystallinity of SWGS significantly decreased with mannitol and xylitol. After four weeks of storage, the SWGS with mannitol and xylitol showed about 25.3% and 27.5% reduction in crystallinity, respectively, indicating that the addition of mannitol and xylitol reduced the crystallinity of SWGS. The V-type characteristic peak was altered, probably due to the formation of a new complex between mannitol and xylitol, amylose, and lipids. In addition, the B-type crystals were produced during staling by the recrystallization of amylopectin and water transfer from the amorphous phase to the crystalline phase [33]. Therefore, it can be inferred that the addition of mannitol and xylitol could minimize the recrystallization of starch by combining with starch through hydrogen bonds. This result was consistent with the infrared experimental results.

3.4. Differential Scanning Calorimetry. Starch, a major structure-forming food hydrocolloid, is composed of amylose, amylopectin, and some small amounts of non-carbohydrate constituents. When starch is heated with excess water, the molecules in the starch granules experience a transition from an ordered to a disordered state, which can be observed using DSC [34].

The changes in the DSC parameters of lyophilized powders stored for 0, 1, 2, 3, and 4 weeks at 4°C with the addition of mannitol and xylitol are presented in Table 2. Here, Tp is the peak temperature of starch retrogradation and ΔH is an important indicator of retrogradation. A larger ΔH indicates more recrystallization, which means more binding between the starch chains, indicating more severe retrogradation. This phenomenon could be attributed to the slow aging of starch molecules at low temperatures, which implies the production of more crystalline or amorphous polymers. Therefore, more energy is needed to break the crystals during the DSC test [14].

Starch retrogradation involves the reassociation and recrystallization of amylose and amylopectin, but amylose retrogradation is quite faster than amylopectin retrogradation [35]. The irreversible crystals were established during amylose retrogradation. When the temperature exceeded 115°C, these crystals could not be remelted, leading to an increase in Tp and ΔH [36]. Compared to the samples without mannitol and xylitol, the samples with mannitol and xylitol showed a significant decrease in Tp and ΔH. The Tp of SWGS stored for 4 weeks with mannitol and xylitol reduced from 133.82°C to 131.93°C and 127.71°C, and the ΔH reduced from 239.4 J/g to 214.0 J/g and 201.0 J/g, respectively. The enthalpy of SWGS stored for 4 weeks at 4°C with xylitol was significantly lower than that of the mannitol sample. Similarly, the enthalpy of SWGS with xylitol was noticeably smaller than that of the samples with mannitol following storage for four weeks at 4°C. This could be attributed to the fact that xylitol contains more hydroxyl groups than mannitol, which could absorb more water and bind to more starch

Table 2: Effects of mannitol and xylitol on the thermal parameters of SWGS storage at different storage times.

Storage time (week)	Samples	T_P (°C)	$\triangle H$ (J/g)
0	Control	120.55 ± 0.44^a	163.2 ± 0.8^a
	Mannitol	119.45 ± 1.47^a	163.4 ± 0.9^a
	Xylitol	117.44 ± 2.12^a	162.0 ± 2.7^a
1	Control	122.97 ± 1.84^a	177.7 ± 2.3^a
	Mannitol	120.79 ± 1.06^a	169.9 ± 1.5^b
	Xylitol	121.06 ± 1.14^a	169.9 ± 1.6^b
2	Control	125.58 ± 1.47^a	210.6 ± 1.1^a
	Mannitol	123.50 ± 1.07^a	181.8 ± 2.4^b
	Xylitol	123.07 ± 1.28^a	167.9 ± 1.3^c
3	Control	129.58 ± 1.51^a	223.9 ± 1.8^a
	Mannitol	127.91 ± 1.27^a	208.6 ± 3.1^b
	Xylitol	126.52 ± 1.42^a	185.8 ± 1.7^c
4	Control	133.82 ± 0.36^a	239.4 ± 1.3^a
	Mannitol	131.93 ± 1.95^a	214.0 ± 1.7^b
	Xylitol	127.71 ± 1.37^b	201.0 ± 2.2^c

Note. Different letters in the same column or line indicate significant differences ($p < 0.05$).

Table 3: Effects of mannitol and xylitol on water distribution and water migration of SWGS at different storage times.

Time/weeks	Samples	T_{21}	T_{22}	T_{23}	R_{21}	R_{22}	R_{23}
0	Control	0.43 ± 0.01^{a}	6.35 ± 0.03^{a}	198.04 ± 9.72^{a}	0.07 ± 0.87^{b}	0.91 ± 0.76^{b}	0.02 ± 0.10^{a}
	Mannitol	0.37 ± 0^{b}	5.92 ± 0.03^{b}	143.76 ± 1.48^{b}	0.08 ± 0.52^{ab}	0.89 ± 0.56^{ab}	0.03 ± 0.04^{a}
	Xylitol	0.36 ± 0.02^{b}	5.66 ± 0.11^{c}	145.16 ± 14.23^{b}	0.09 ± 0.40^{a}	0.88 ± 0.85^{a}	0.03 ± 0.45^{a}
1	Control	0.39 ± 0.01^{a}	5.96 ± 0.03^{a}	170.60 ± 5.96^{a}	0.05 ± 0.03^{b}	0.93 ± 0.18^{a}	0.03 ± 0.14^{a}
	Mannitol	0.34 ± 0.01^{c}	5.61 ± 0.08^{b}	140.80 ± 7.89^{b}	0.06 ± 0.34^{a}	0.91 ± 1.03^{b}	0.03 ± 0.69^{a}
	Xylitol	0.34 ± 0.01^{c}	5.58 ± 0.09^{b}	133.22 ± 2.83^{b}	0.06 ± 0.74^{a}	0.91 ± 0.40^{ab}	0.03 ± 0.35^{a}
2	Control	0.37 ± 0.01^{a}	5.81 ± 0.10^{a}	162.24 ± 4.04^{a}	0.04 ± 0.40^{b}	0.93 ± 0.55^{a}	0.02 ± 0.15^{a}
	Mannitol	0.36 ± 0.02^{a}	5.51 ± 0.05^{b}	131.63 ± 4.64^{b}	0.05 ± 0.17^{a}	0.92 ± 0.09^{a}	0.03 ± 0.26^{a}
	Xylitol	0.35 ± 0.01^{a}	5.40 ± 0.07^{b}	136.58 ± 11.65^{b}	0.05 ± 0.14^{a}	0.92 ± 0.61^{a}	0.03 ± 0.47^{a}
3	Control	0.37 ± 0.01^{a}	5.60 ± 0.04^{a}	156.20 ± 1.96^{a}	0.04 ± 0.16^{b}	0.93 ± 0.45^{a}	0.02 ± 0.29^{a}
	Mannitol	0.33 ± 0.02^{ab}	5.20 ± 0.04^{bc}	123.37 ± 2.62^{c}	0.05 ± 0.07^{a}	0.92 ± 0.15^{b}	0.03 ± 0.08^{a}
	Xylitol	0.31 ± 0.01^{b}	5.02 ± 0.14^{c}	120.53 ± 4.16^{c}	0.05 ± 0.29^{a}	0.92 ± 0.09^{b}	0.03 ± 0.21^{a}
4	Control	0.36 ± 0.01^{a}	5.55 ± 0.07^{a}	139.29 ± 8.75^{a}	0.04 ± 0.09^{b}	0.94 ± 0.26^{a}	0.02 ± 0.18^{b}
	Mannitol	0.32 ± 0.01^{bc}	5.08 ± 0.06^{bc}	110.57 ± 6.41^{bc}	0.05 ± 0.04^{a}	0.93 ± 0.20^{bc}	0.02 ± 0.16^{a}
	Xylitol	0.32 ± 0.01^{c}	4.87 ± 0.07^{c}	107.28 ± 2.54^{c}	0.05 ± 0.08^{a}	0.92 ± 0.13^{c}	0.03 ± 0.05^{a}

Note. Different letters in the same column or line indicate significant differences ($p < 0.05$).

molecules. Therefore, adding xylitol could effectively inhibit the retrogradation of SWGS [37].

3.5. Low-Field Nuclear Magnetic Resonance. LF-NMR is a potential approach to investigate water distribution and migration. In this study, starch water transportation during the retrogradation process was detected by LF-NMR. The degree of freedom of water was reflected by the T_2 relaxation time. Table 3 shows the T_2 relaxation times of SWGS at different storage times. The composition of the water in T_2 is subdivided into three categories. The spin relaxation time of T_{21} was between 0.1 and 1 ms, and in this range, molecules of water were bounded to the starch in the SWGS by hydrogen bonding, which was known as bound water. The spin relaxation time of T_{22} was between 1 and 10 ms. The water molecules in this range were poorly bound to the starch, which makes it incredibly hard for them to flow. T_{23} exhibited spin relaxation times between 10 ms and 1000 ms. The water molecules in this range were not intimately linked to the starch; instead, they were attached to the surface of the gel structure, which is called free water [38].

It can be seen from Table 3 that the T_{21}, T_{22}, and T_{23} of all the samples significantly decreased with the increase in storage time. The extent of binding of water molecules in the sample was observed by the spin relaxation time, and the tight binding of water molecules in the sample was observed by the lower spin relaxation time. These results suggested that the interaction between starch and water molecules enhanced and the fluidity of water restricted with increased storage time. Therefore, the retrograded starch gel formed a denser structure. The addition of mannitol and xylitol resulted in a noticeable reduction in the T_{21}, T_{22}, and T_{23} relaxation times, indicating that the synergistic interplay among mannitol, xylitol, and starch facilitated the formation of more ordered structures, leading to stronger binding of the starch molecules to the water molecules. In the early stage of gel storage, the content of free water in the gel was the highest, so the water loss was the largest. However, the water loss of the gel was reduced with the addition of mannitol and xylitol. The interaction among mannitol, xylitol, and starch enabled the starch to combine with more water [39] molecules [15]. The decrease in T_{21} and T_{22} was not significant, but the decrease in T_{23} was extremely significant. The result indicated that the concentration of mannitol and xylitol had no obvious effect on the migration of bound water and immobile water but could effectively reduce the migration of free water [39]. The fluidity of water was limited, the mobility of starch molecules was weak, and the recrystallization of the starch chain was reduced. So, the starch retrogradation was inhibited [40], which could be attributed to the structure of mannitol and xylitol.

The proportion of each component of water is represented by R_{21}, R_{22}, and R_{23}, respectively. The moisture in the SWGS was mostly in the form of immobile water, and the ratio of the moisture content of the components did not vary regularly, which might be attributed to the fact that the moisture in the samples was subjected to a dynamic migration process.

4. Conclusion

In this study, the retrogradation characteristics of SWGS stored at different storage times with 2% mannitol and 4% xylitol were investigated. The following conclusions were obtained: (1) the addition of 2% mannitol and 4% xylitol significantly reduced the hardness, T_p, and ΔH of SWGS. Moreover, the addition of xylitol significantly reduced the rate of retrogradation in SWGS. (2) The addition of polyol significantly reduced the T_2 relaxation time, thereby enhancing the binding of water molecules. Overall, these results indicate that the addition of 2% mannitol and 4% xylitol, especially xylitol, could have positive and improving effects on the antiretrogradation of SWGS.

Data Availability

The data used to support the findings of this study are included within this article.

Conflicts of Interest

The authors declare that they have no conflicts of interest.

Acknowledgments

The work was financially supported by the Science and Technology Development Project of National Guided Local Hubei Provincial, China (No. 2019ZYYD036).

References

[1] J. M. Awika, "Major cereal grains production and use around the world," in *Advances in Cereal Science: Implications to Food Processing and Health Promotion*, vol. 1089, pp. 1–13, American Chemical Society, Washington, DC, USA, 2011.

[2] X. Hu, L. Hu, J. Zheng, and J. Rong, "Classification, processing procedures, and market demand of Chinese biscuits and the breeding of special wheat for biscuit making," *Journal of Food Quality*, vol. 2022, Article ID 6679776, 12 pages, 2022.

[3] N. Lakshmi Devi, S. Shobha, S. Alavi, K. Kalpana, and M. Soumya, "Utilization of extrusion technology for the development of millet based complementary foods," *Journal of Food Science and Technology*, vol. 51, no. 10, pp. 2845–2850, 2014.

[4] S. Agrawal, R. K. Raigar, and H. N. Mishra, "Effect of combined microwave, hot air, and vacuum treatments on cooking characteristics of rice," *Journal of Food Process Engineering*, vol. 42, no. 4, 2019.

[5] J. Zhou, H. Yang, X. Qin, X. Hu, G. Liu, and X. Wang, "Effect of β-cyclodextrin on the quality of wheat flour dough and prebaked bread," *Food Biophysics*, vol. 14, no. 2, pp. 173–181, 2019.

[6] Y. Fu, X. Liu, Q. Xie et al., "Effects of Laminaria japonica polysaccharides on the texture, retrogradation, and structure performances in frozen dough bread," *LWT-Food Science and Technology*, vol. 151, Article ID 112239, 2021.

[7] Y. Wu, M. Niu, and H. Xu, "Pasting behaviors, gel rheological properties, and freeze-thaw stability of rice flour and starch modified by green tea polyphenols," *LWT-Food Science and Technology*, vol. 118, Article ID 108796, 2020.

[8] M. Ma, C.-W. Han, M. Li, X.-Q. Song, Q.-J. Sun, and K.-X. Zhu, "Inhibiting effect of low-molecular weight polyols on the physico-chemical and structural deteriorations of gluten protein during storage of fresh noodles," *Food Chemistry*, vol. 287, pp. 11–19, 2019.

[9] S. Ding, B. Peng, Y. Li, and J. Yang, "Evaluation of specific volume, texture, thermal features, water mobility, and inhibitory effect of staling in wheat bread affected by maltitol," *Food Chemistry*, vol. 283, pp. 123–130, 2019.

[10] H. Yang, M. Tang, W. Wu, W. Ding, B. Ding, and X. Wang, "Study on inhibition effects and mechanism of wheat starch retrogradation by polyols," *Food Hydrocolloids*, vol. 121, Article ID 106996, 2021.

[11] H. İspirli, D. Özmen, M. T. Yılmaz, O. Sağdıç, and E. Dertli, "Impact of glucan type exopolysaccharide (EPS) production on technological characteristics of sourdough bread," *Food Control*, vol. 107, Article ID 106812, 2020.

[12] B. Zhu, J. Zhan, L. Chen, and Y. Tian, "Amylose crystal seeds: preparation and their effect on starch retrogradation," *Food Hydrocolloids*, vol. 105, Article ID 105805, 2020.

[13] Y. Zhang, C. Chen, Y. Chen, and Y. Chen, "Effect of rice protein on the water mobility, water migration and microstructure of rice starch during retrogradation," *Food Hydrocolloids*, vol. 91, pp. 136–142, 2019.

[14] Y. Liu, X. Zhang, B. Ding et al., "Effect of hydrocolloids on physical, thermal and microstructure properties of par-baked baguette during frozen storage," *International Journal of Biological Macromolecules*, vol. 163, pp. 1866–1874, 2020.

[15] H. Niu, M. Zhang, X. Xia, Q. Liu, and B. Kong, "Effect of porcine plasma protein hydrolysates on long-term retrogradation of corn starch," *Food Chemistry*, vol. 239, pp. 172–179, 2018.

[16] A. Asghar, F. M. Anjum, M. S. Butt, M. A. Randhawa, and S. Akhtar, "Effect of polyols on the rheological and sensory parameters of frozen dough pizza," *Food Science and Technology Research*, vol. 18, no. 6, pp. 781–787, 2012.

[17] N. Pematilleke, M. Kaur, B. Adhikari, and P. Torley, "Influence of meat texture on oral processing and bolus formation," *Journal of Food Engineering*, vol. 283, Article ID 110038, 2020.

[18] W. W. Kim and B. Yoo, "Rheological and thermal effects of galactomannan addition to acorn starch paste," *LWT-Food Science and Technology*, vol. 44, no. 3, pp. 759–764, 2011.

[19] S. Wang, C. Li, L. Copeland, Q. Niu, and S. Wang, "Starch retrogradation: a comprehensive review," *Comprehensive Reviews in Food Science and Food Safety*, vol. 14, no. 5, pp. 568–585, 2015.

[20] J. Pan, M. Li, S. Zhang et al., "Effect of epigallocatechin gallate on the gelatinisation and retrogradation of wheat starch," *Food Chemistry*, vol. 294, pp. 209–215, 2019.

[21] Q. Sun, L. Dai, C. Nan, and L. Xiong, "Effect of heat moisture treatment on physicochemical and morphological properties of wheat starch and xylitol mixture," *Food Chemistry*, vol. 143, pp. 54–59, 2014.

[22] L. S. Sciarini, M. C. Bustos, M. B. Vignola, C. Paesani, C. N. Salinas, and G. T. Pérez, "A study on fibre addition to gluten free bread: its effects on bread quality and in vitro digestibility," *Journal of Food Science and Technology*, vol. 54, no. 1, pp. 244–252, 2017.

[23] L. Chen, F. Ren, Z. Zhang, Q. Tong, and M. M. A. Rashed, "Effect of pullulan on the short-term and long-term retrogradation of rice starch," *Carbohydrate Polymers*, vol. 115, pp. 415–421, 2015.

[24] Y. Yao, J. Zhang, and X. Ding, "Structure-retrogradation relationship of rice starch in purified starches and cooked rice grains: a statistical investigation," *Journal of Agricultural and Food Chemistry*, vol. 50, no. 25, pp. 7420–7425, 2002.

[25] Y. Tian, Y. Li, X. Xu, and Z. Jin, "Starch retrogradation studied by thermogravimetric analysis (TGA)," *Carbohydrate Polymers*, vol. 84, no. 3, pp. 1165–1168, 2011.

[26] Ö. Koyuncu, N. BilgiÇLi, A. ElgÜN, and M. Kara, "Effect of pentosanase on dough and bread properties produced by different types of flours," *Journal of Food Quality*, vol. 31, no. 2, pp. 156–172, 2008.

[27] C. Pozo, S. Rodríguez-Llamazares, R. Bouza et al., "Study of the structural order of native starch granules using combined FTIR and XRD analysis," *Journal of Polymer Research*, vol. 25, no. 12, p. 266, 2018.

[28] W. Li, C. Li, Z. Gu et al., "Retrogradation behavior of corn starch treated with 1,4-α-glucan branching enzyme," *Food Chemistry*, vol. 203, pp. 308–313, 2016.

[29] S. Ding and J. Yang, "The effects of sugar alcohols on rheological properties, functionalities, and texture in baked products-a review," *Trends in Food Science & Technology*, vol. 111, pp. 670–679, 2021.

[30] J. Xiong, Q. Li, Z. Shi, and J. Ye, "Interactions between wheat starch and cellulose derivatives in short-term retrogradation: rheology and FTIR study," *Food Research International*, vol. 100, pp. 858–863, 2017.

[31] X. Wu, H. Yu, G. Bao, M. Luan, and C. Wang, "Preparation of adzuki bean starch-lipid complexes and their anti-digestion mechanism," *Journal of Food Measurement and Characterization*, vol. 16, no. 2, pp. 945–956, 2022.

[32] W. Li, F. Cao, J. Fan et al., "Physically modified common buckwheat starch and their physicochemical and structural properties," *Food Hydrocolloids*, vol. 40, pp. 237–244, 2014.

[33] I. Demirkesen, O. H. Campanella, G. Sumnu, S. Sahin, and B. R. Hamaker, "A study on staling characteristics of gluten-free breads prepared with chestnut and rice flours," *Food and Bioprocess Technology*, vol. 7, no. 3, pp. 806–820, 2014.

[34] P. Kaur, M. Singh, and P. Birwal, "Differential scanning calorimetry (DSC) for the measurement of food thermal characteristics and its relation to composition and structure," in *Techniques to Measure Food Safety and Quality: Microbial, Chemical, and Sensory*, M. S. Khan and M. Shafiur Rahman, Eds., Springer International Publishing, Cham, Switzerland, pp. 283–328, 2021.

[35] A. C. Eliasson, "10-gelatinization and retrogradation of starch in foods and its implications for food quality," in *Chemical Deterioration and Physical Instability of Food and Beverages*, L. H. Skibsted, J. Risbo, and M. L. Andersen, Eds., Woodhead Publishing, Sawston, UK, pp. 296–323, 2010.

[36] H. Yang, Y. Fu, Y. Zhang et al., "Evaluation of mannitol and xylitol on the quality of wheat flour and extruded flour products," *International Journal of Food Science and Technology*, vol. 56, no. 8, pp. 4119–4128, 2021.

[37] S. Y. J. Sim and C. I. Moraru, "High-pressure processing of pea protein–starch mixed systems: effect of starch on structure formation," *Journal of Food Process Engineering*, vol. 43, no. 2, 2020.

[38] L. Chen, Y. Tian, Q. Tong, Z. Zhang, and Z. Jin, "Effect of pullulan on the water distribution, microstructure and textural properties of rice starch gels during cold storage," *Food Chemistry*, vol. 214, pp. 702–709, 2017.

[39] Y. Luo, X. Han, M. Shen, J. Yang, Y. Ren, and J. Xie, "Mesona chinensis polysaccharide on the thermal, structural and digestibility properties of waxy and normal maize starches," *Food Hydrocolloids*, vol. 112, Article ID 106317, 2021.

[40] C. Ma, C. Tan, J. Xie et al., "Effects of different ratios of mannitol to sorbitol on the functional properties of sweet potato starch films," *International Journal of Biological Macromolecules*, vol. 242, Article ID 124914, 2023.